

Solution Properties and Chain Stiffness of (Cyanoethyl)(hydroxypropyl)cellulose

Jimmy W. Mays¹

Hercules Incorporated, Research Center, Wilmington, Delaware 19894.

Received October 25, 1987; Revised Manuscript Received April 20, 1988

ABSTRACT: The length of the Kuhn statistical segment, l' , for (cyanoethyl)(hydroxypropyl)cellulose (CEHPC) was evaluated from combined intrinsic viscosity-molecular weight data using the method of Bohdanecky. A series of eight fractionated CEHPC samples having weight-average molecular weights between 5.3×10^4 and 2.69×10^5 were employed for this purpose. The Kuhn length was found to equal 286 Å; this value is somewhat higher than values of l' found for most other cellulose derivatives. Critical volume fractions for mesophase formation, V_2^* , were calculated from the aspect ratio of the Kuhn segment by using the theory of Flory. The theoretical value of 0.35 was found to be in excellent accord with that value, 0.34, obtained by polarizing microscopy. In addition, the temperature quotient was evaluated from intrinsic viscosity measurements over the range of 25–75 °C. A large negative value of $-3.8 \times 10^{-3} \text{ K}^{-1}$ was found for $d \ln \langle r^2 \rangle_0 / (M)_\infty / dT$.

Introduction

(Cyanoethyl)(hydroxypropyl)cellulose (CEHPC) is a relatively new organosoluble cellulose derivative prepared by reaction of acrylonitrile with (hydroxypropyl)cellulose (HPC) under alkaline conditions. CEHPC is chemically characterized in terms of both molar substitution (MS) of propylene oxide and degree of substitution (DS) of cyanoethyl groups. At appropriate substitution levels CEHPC is soluble in a variety of organic solvents including tetrahydrofuran (THF), acetone, butanone, Cellosolve (trademark of Union Carbide Corp.), ethyl acetate, acrylonitrile, and *N,N*-dimethylacetamide (DMAC). An idealized structure of CEHPC is shown in Figure 1.

The tendency of cellulose and cellulose derivatives to form liquid crystals in concentrated solutions is now well-documented.^{2–10} The primary requirement for liquid crystal formation is asymmetry of molecular shape.¹¹ In this paper, we report the determination of Kuhn statistical segment lengths and chain diameters for CEHPC, which forms cholesteric liquid crystals. From the aspect ratio of the Kuhn segment, the critical volume fraction (V_2^*) of CEHPC necessary for mesophase formation is calculated by using the theory of Flory.^{11,12} Calculated values of V_2^* are compared with experimentally derived values.

Theory

Cellulose derivatives have flexibilities intermediate between rigid rod and random coil structures. A convenient and useful model for studying the configurations of such chains is the wormlike chain model.¹³ Wormlike chains are characterized by a contour length, L , a diameter, d , and persistence length, q . The Kuhn length, l' , is related to q by the equation

$$l' = 2q \quad (1)$$

Benoit and Doty¹⁴ have shown that q can be derived from the polymer radius of gyration, $\langle S^2 \rangle$, by the equation

$$\langle S^2 \rangle = q^2 [1/3(L/q) - 1 + (2q/L) - (2q^2/L^2)[1 - \exp(-L/q)]] \quad (2)$$

Alternatively, a number of approaches^{15–21} have been developed for deriving parameters of wormlike chains from hydrodynamic quantities such as the intrinsic viscosity.

Perhaps the most widely accepted of these latter approaches is the theory of Yamakawa and Fujii.²⁰ Bohdanecky²² has recently developed a simple graphical procedure based on the Yamakawa-Fujii equation

$$[\eta]_0 = \Phi_0 (l')^{3/2} L^{1/2} / M_L \quad (3)$$

where $[\eta]_0$ is the unperturbed intrinsic viscosity, Φ_0 is the hydrodynamic parameter, and $M_L = M/L$ where M is molecular weight. The value of Φ_0 depends on L_r and d_r where $L_r = L/l'$ and $d_r = d/l'$. Φ_0 takes on the limiting theoretical value for flexible coils in the limit of $L_r \rightarrow \infty$.²⁰ We have chosen to use $\Phi_{0,\infty} = 2.86 \times 10^{23}$, since this is the value preferred by Bohdanecky. Bohdanecky has demonstrated²² that Φ_0 can be given a simple form

$$\Phi_0 = \Phi_{0,\infty} [B_0 + A_0 (l'/L)^{1/2}]^{-3} \quad (4)$$

where B_0 is essentially constant and A_0 is a function of d_r .

The final form of the Bohdanecky equation is

$$(M^2/[\eta]_0)^{1/3} = A_\eta + B_\eta M^{1/2} \quad (5)$$

where

$$A_\eta = A_0 M_L \Phi_{0,\infty}^{-1/3} \quad (6)$$

and

$$B_\eta = B_0 \Phi_{0,\infty}^{-1/3} (\langle r^2 \rangle_0 / M)_\infty^{-1/2} \quad (7)$$

$\langle r^2 \rangle_0$ is the unperturbed mean-square end-to-end distance, and the subscript ∞ denotes that the $\langle r^2 \rangle_0 / M$ value obtained from B_η is the random coil value. A plot of $(M^2/[\eta]_0)^{1/3}$ versus $M^{1/2}$ is expected to be linear, and $(\langle r^2 \rangle_0 / M)_\infty$ is derived from the slope. The Kuhn length is calculated as $l' = \langle r^2 \rangle_0 / N l_u$ where $N = M/M_u$, M_u is the molecular weight of the repeating unit, and l_u is the length of the repeating unit projected on the molecular axis.

Chain diameters can also be evaluated from the Bohdanecky plot if the partial specific volume, ν , of the polymer is known. Bohdanecky²² has shown that

$$(d_r^2/A_0) = (4\Phi_{0,\infty}/1.215\pi N_A)(\nu/A_\eta)B_\eta^4 \quad (8)$$

where values of (d_r^2/A_0) have been empirically established²² as a function of d_r .

$$\log (d_r^2/A_0) = 0.173 + 2.158 \log d_r \quad (9)$$

Equation 9 is valid for $d_r \leq 0.1$, and d can be calculated directly from eq 9 since $d = d_r l'$.

Very recently, Reddy and Bohdanecky²³ have derived a method for estimating the temperature quotient of chain dimensions, $d \ln \langle r^2 \rangle_0 / (M)_\infty / dT$, from the temperature quotient of the intrinsic viscosity, $d \ln [\eta] / dT$, of stiff chain polymers. Their approach again utilizes the Yamakawa-Fujii wormlike cylinder model.²⁰ If $d \ln [\eta] / dT$ is independent of molecular weight, the following simple equation was derived.²³

$$d \ln \langle r^2 \rangle_0 / (M)_\infty / dT = 2/3 d \ln [\eta] / dT \quad (10)$$

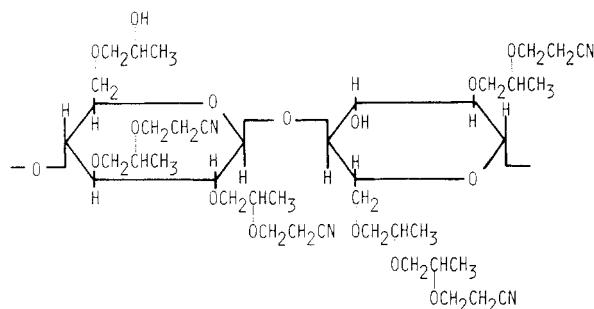


Figure 1. Idealized structure for CEHPC with $MS = 3.0$ and $DS = 2.0$. The CEHPC fractions studied in this work have $MS = 3.88$ and $DS = 2.75$.

Experimental Section

The CEHPC sample used in this work was prepared from Klucel LF hydroxypropylcellulose, a product of the Aqualon Group, by Dr. P. E. Barnum of Hercules Incorp. The synthesis was carried out by slowly adding 5% sodium hydroxide to a solution of (hydroxypropyl)cellulose in excess acrylonitrile with stirring. Reaction took place for 4 h at 45–50 °C. The reaction mixture was neutralized, and the product was precipitated into methanol. The substitution of the parent HPC was determined by the terminal methyl group method of Lemieux and Purves;²⁴ MS was found to equal 3.9.

Fractionation was carried out by incremental addition of *n*-heptane to a 1% solution of CEHPC in acetone. Ten fractions were obtained by this procedure. Nitrogen contents of six fractions were measured by the Kjeldahl method. These results showed uniform DS of cyanoethyl functionality for all but the first two fractions, that is, the two highest molecular weight fractions. These materials were found to have lower degrees of cyanoethyl substitution. DS values for the other fractions were found to equal 2.75 ± 0.2 . MS determinations yielded values equal to 3.88 ± 0.1 . These latter data support the conclusions of Wirick and Waldman²⁵ that substitution of HPC is essentially uniform across the molecular weight distribution. These results also suggest that fractionation of CEHPC, using acetone/*n*-heptane mixtures, proceeds initially on the basis of molecular weight and DS . Subsequent fractionation is probably based only on molecular weight differences.

Size exclusion chromatography (SEC) results were obtained for the "parent" CEHPC sample and the fractions. A Waters ALC/GPC 201 unit was employed by using THF as the mobile phase at 25 °C. A μ -Styragel column set, having porosities of 5×10^2 , 10^3 , 10^4 , 10^5 , and 10^6 Å, was used for the separation with a differential refractive index detector being employed. Calibration was based on near-monodisperse polystyrene standards.

Low-angle laser light scattering (LALLS) was employed for the determination of weight-average molecular weights (\bar{M}_w) and second virial coefficients (A_2). Distilled-in-glass grade THF from Burdick and Jackson was used as the solvent. Measurements were conducted at 25 °C by using a Chromatix KMX-6 photometer at 6328 Å. Specific refractive index increments (dn/dc) were measured under the same conditions by using the Chromatix KMX-16 differential refractometer. A value of 0.0818 mL g^{-1} was obtained for the unfractionated sample; this value was employed in measuring \bar{M}_w and A_2 of the fractions.

Intrinsic viscosity measurements were carried out by using Cannon–Ubbelohde viscometers with negligible kinetic energy corrections. Thermal control of the water bath was maintained to ± 0.02 °C with a Haake E-3 heater/circulator. Distilled-in-glass THF (Burdick and Jackson) and DMAC (Aldrich, 99.9+%) were used as received. Four or five concentrations of polymer were used for obtaining the intrinsic viscosity and Huggins coefficients from a linear regression fit of η_{sp}/c versus c .

X-ray diffraction measurements on a liquid crystalline solution of CEHPC in THF (ca. 50% (w/w)), in a wax-sealed, thin-walled capillary, were carried out by Dr. Nikos Pyrras of Hercules Incorp. A Philips ADP 3600 X-ray diffractometer with X-ray diffraction flat plate photographs was employed.

Partial specific volumes of CEHPC in THF and HPC in absolute ethanol were calculated from density measurements on

Table I
SEC Analysis of CEHPC Fractions

sample	\bar{M}_w/\bar{M}_n	\bar{M}_z/\bar{M}_w	sample	\bar{M}_w/\bar{M}_n	\bar{M}_z/\bar{M}_w
parent	2.67	2.64	F-6	1.42	1.44
F-1	3.79	1.97	F-7	1.38	1.48
F-2	2.61	1.82	F-8	1.32	1.51
F-3	2.30	1.79	F-9	1.29	1.47
F-4	1.89	1.76	F-10	1.20	1.22
F-5	1.63	1.70			

Table II
Molecular Characteristics of CEHPC in THF at 25 °C

sample	$10^{-4}\bar{M}_w$, g mol ⁻¹	$10^4 A_2$, mL mol g ⁻²	$[\eta]$, mL g ⁻¹	k_H
F-3	26.9	3.7	252	0.49
F-4	17.3	4.7	182	0.50
F-5	12.4	4.5	140	0.49
F-6	11.0	4.6	108	0.52
F-7	8.92	3.8	93.5	0.65
F-8	7.91	4.3	80.8	0.58
F-9	6.40	3.6	61.1	0.67
F-10	5.35	4.0	54.4	0.37

solvent and polymer solutions. These densities were obtained at 25 °C by using a Mettler/Par Model DMA 46 digital density meter. Values of 0.783 and 0.819 mL g^{-1} were found for solutions of CEHPC and HPC, respectively. The bulk density of CEHPC was measured by displacement, using ASTM Method D792-66. *n*-Heptane (Burdick and Jackson, distilled-in-glass) was used as the displacement fluid. Heptane wet the CEHPC surface, yet a sample of CEHPC left in *n*-heptane for 1 month showed no signs of swelling. A value of 1.14 g mL^{-1} was obtained at 20 °C.

The threshold volume fraction, V_2^* , for CEHPC in THF was determined by observing solutions of different concentrations with an Olympus BH-2 microscope under crossed-polarized light. Solutions were initially prepared on a weight-to-weight basis. These concentrations were corrected to volume fractions by using the partial specific volume of CEHPC in THF and the specific volume of THF and assuming additivity. Solutions having concentrations above V_2^* were birefringent under crossed polarizers (Figure 2).

At polymer concentrations much greater than V_2^* ($\geq 70\%$) iridescent solutions, characteristic of a cholesteric mesophase, are obtained. This behavior is reminiscent of the behavior noted previously^{2,3} for solutions of HPC. The light reflected by CEHPC solutions varied from red to green to blue, etc., depending on the point of observation.

Results and Discussion

SEC results for CEHPC fractions (F-1 was the first fraction taken and F-10 was taken last) and the unfractionated "parent" material are summarized in Table I. The values of \bar{M}_w/\bar{M}_n and \bar{M}_z/\bar{M}_w reported here should be considered estimates, since they are based on a polystyrene calibration. Ambler and co-workers^{26,27} have demonstrated that the conventional universal calibration approach is not necessarily applicable when species with dissimilar molecular geometries are involved. Even so, it appears that F-1 actually has higher polydispersity than that found for the parent material. This result is likely caused by "cross-fractionation", as noted in the Experimental Section.²⁸ Also, polydispersity appears to decrease with each successive fraction that was taken. This is to be expected, since decreasing polymer concentration and decreasing \bar{M}_w of the polymer remaining in solution yields more efficient fractionations.²⁹

The \bar{M}_w and $[\eta]$ data of Table II yield the following Mark–Houwink–Sakurada (M–H–S) relation

$$[\eta]_{\text{THF}}^{25^\circ\text{C}} = 1.14 \times 10^{-3} \bar{M}_w^{0.99} \quad (11)$$

These data are also plotted in Figure 3. The value of the M–H–S exponent is very close to one, in agreement with

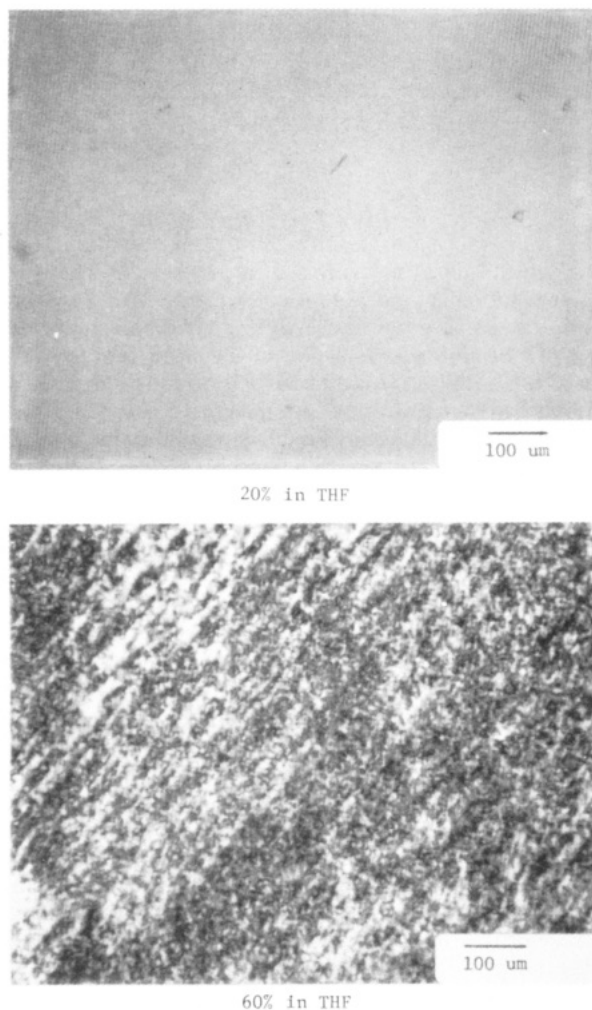


Figure 2. Photomicrographs of CEHPC solutions under crossed polarizers. Magnification is 84 \times . The 60% (w/w) solution of CEHPC in THF exhibits a strongly birefringent pattern. No birefringence is observed for the 20% (w/w) solution.

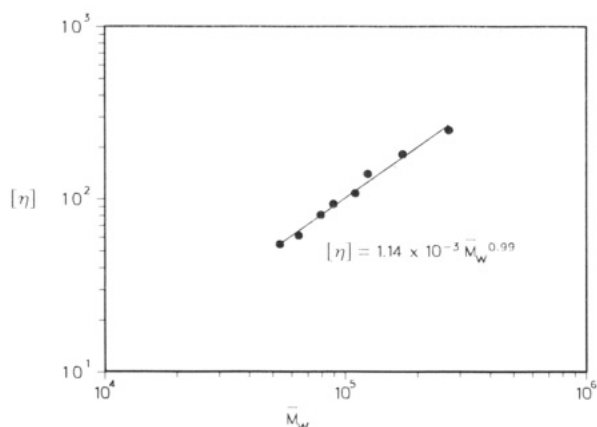


Figure 3. Mark-Houwink-Sakurada plot for CEHPC in THF.

results for cellulose and cellulose derivatives where values between 0.8 and 1.0 are usually found.³⁰ The M-H-S exponent of unity eliminates the need for polydispersity corrections that are normally required when comparing a viscosity-average measure of size with a weight-average molecular weight, since Flory has shown that $\bar{M}_v = \bar{M}_w$ under these conditions.³¹

The Bohdanecky plot for CEHPC in THF is given in Figure 4. The parameters A_η and B_η were evaluated from the intercept and slope, respectively, and were used in calculating l' and d as outlined above. \bar{M}_u was calculated

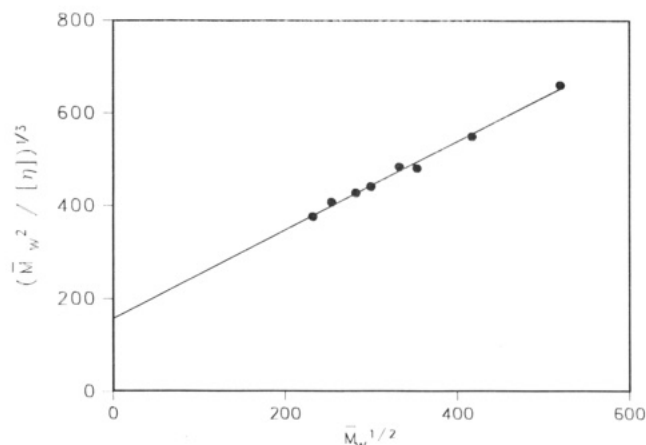


Figure 4. Bohdanecky plot for CEHPC in THF.

Table III
Kuhn Lengths and Chain Diameters for CEHPC and HPC

polymer	l' , Å	d , Å
CEHPC	286	13.8
HPC	274	9.2

Table IV
Chain Diameters of CEHPC and HPC

polymer	d , Å	method	ref
CEHPC	13.8	viscosity	this work
CEHPC	12.3	density	this work
CEHPC	15.2	X-ray	this work
HPC	9.8	viscosity	this work
HPC	9.5	density	11
HPC	12.8	X-ray	3

as 533 g mol⁻¹, and l_u was taken as 5.14 Å.³²

The values of l' and d are given in Table III for CEHPC in THF and HPC in ethanol. The results for HPC in ethanol are based on \bar{M}_w and $[\eta]$ results reported by Wirick and Waldman.²⁵ The Bohdanecky approach yields essentially the same Kuhn length for CEHPC as for HPC, but the diameter of CEHPC is larger as expected due to its greater level of substitution.

It is relevant to note that no corrections for excluded volume were applied to the viscosity data. While Θ conditions are unknown for CEHPC and thus a direct measure of excluded volume effects is not possible, these effects have been demonstrated to be quite small for cellulose and cellulose derivatives.³³⁻³⁵ Norisuye and Fujita³⁵ have also shown that the onset of the excluded volume effect occurs at a critical chain length of about 100 q , a value which far exceeds the length of the samples used in this work. Thus, the decision to ignore chain expansion appears to be well justified.

It is of interest to compare the values of d obtained by the Bohdanecky approach with values of d obtained by other methods. Flory¹¹ has put forth a method based on bulk density, ρ , of the polymer

$$d = (M_u / \rho N_a l_u)^{1/2} \quad (12)$$

where N_a is Avogadro's number. In addition, X-ray diffraction studies on concentrated solutions ($c > V_2^*$) or the bulk mesophase are useful in deducing the distance between the axes of the molecules.³

Results for chain diameters of CEHPC and HPC are given in Table IV. Values from X-ray diffraction measurements on concentrated solutions of HPC³ and CEHPC are found to be somewhat larger than values obtained by the viscosity and bulk density methods. These results are not surprising, since the addition of solvent would be ex-

Table V
Comparison of Theoretical and Experimental Values of V_2^* for Cellulose Derivatives

derivative	solvent	X	V_2^* (theory)	V_2^* (exptl)	ref
CEHPC	THF	20.7	0.35	0.34	this work
HPC	ethanol	25.6	0.29	0.38	3, this work
CA	CF ₃ COOH	26	0.28	0.25	11
EC	various	23	0.32	0.34	11
APC	dimethyl phthalate	11.5	0.57	0.52	38, 39

Table VI
Intrinsic Viscosity as a Function of Temperature for CEHPC Fractions in DMAC

sample	$[\eta]_{25^\circ\text{C}}$ mL g ⁻¹	k_H	$[\eta]_{50^\circ\text{C}}$ mL g ⁻¹	k_H	$[\eta]_{75^\circ\text{C}}$ mL g ⁻¹	k_H
F-3	235	0.38	210	0.35	176	0.42
F-4	180	0.34	158	0.34	136	0.32
F-5	141	0.33	123	0.35	107	0.36

pected to lead to greater spacing between the molecular axes.³⁷ The viscosity and bulk density methods give values that are in good agreement with one another.

For subsequent calculations, an average of the three determinations will be taken, that is, d is taken as 13.8 and 10.7 Å for CEHPC and HPC, respectively. The larger average value of d for CEHPC is to be expected in view of the presence of additional substituents on the anhydroglucose repeating units.

Threshold volume fractions for CEHPC and HPC were calculated from the data in Tables III and V by using the equation of Flory¹²

$$V_2^* = (8/X)(1 - 2/X) \quad (13)$$

where $X = l'/d$.¹¹ Results are given in Table V, along with results for cellulose acetate (CA), (acetoxypentyl)cellulose (APC), and ethylcellulose (EC). These values are compared with experimentally determined values of V_2^* , that is, results based on observation of a stable mesophase under crossed polarizers or other suitable methods.

In general, it is seen from Table V that calculated and theoretical values of V_2^* are in good agreement, with the exception of results for HPC in ethanol. We are unable to explain this anomalous behavior for HPC, but the potential does exist for hydrogen bonding in this system. Hydrogen bonding and other "soft" intermolecular interactions, which have been discussed by Flory,¹¹ can exert an influence on the phase behavior. It is also pertinent to mention that l' for HPC has been found to show a strong dependence on the choice of solvent.^{3,25,40,41}

The temperature dependence of $[\eta]$ for CEHPC samples F-3, F-4, and F-5 in DMAC is given in Table VI. The values of $[\eta]$ at 25 °C in DMAC are quite close to those reported in THF at the same temperature (Table II). Thus, specific solvent effects appear to be negligible for CEHPC solutions, at least insofar as dilute solution behavior in THF and DMAC is concerned.

On increasing temperature, a large decrease in $[\eta]$ is observed. This suggests a large decrease in chain stiffness for CEHPC with increasing temperature. The temperature coefficient of the intrinsic viscosity, $d \ln [\eta]/dT$, is reported for each of the three CEHPC fractions in Table VII. Only a very slight molecular weight dependence is observed, and it is felt that the differences are not significant within experimental errors. Consequently, eq 10 was employed for calculating $d \ln (\langle r^2 \rangle_0/M_\infty)/dT$. A value of $-3.8 \times 10^{-3} \text{ K}^{-1}$ is obtained. Large negative temperature coefficients like the one reported here are typical for cellulose derivatives^{42,43} and stiff chain polymers in general.²³

Table VII
Temperature Coefficients of Intrinsic Viscosity for CEHPC Fractions

sample	$10^3 d \ln [\eta]/dT, \text{ K}^{-1}$	$10^{-4} \bar{M}_w, \text{ g mol}^{-1}$
F-3	-5.78	26.9
F-4	-5.61	17.3
F-5	-5.52	12.4

From a practical standpoint, the above results indicate that caution must be exercised in processing liquid crystalline solutions at elevated temperatures. In other words, solutions that are liquid crystalline at room temperature may not be liquid crystalline at elevated temperatures, since the reduction in unperturbed dimensions would be expected to be manifested in a decreased aspect ratio and increased V_2^* . Conversely, liquid crystallinity may possibly be induced in isotropic solutions by reducing the temperature.

Finally, we note that neither A_2 nor k_H shows (within experimental error) any dependence on molecular weight for CEHPC fractions. Surprisingly, the Huggins coefficients found in THF were greater than the value found in DMAC at 25 °C despite the fact that no specific solvent effect on $[\eta]$ was observed. Also, the data of Table VI indicate no dependence of k_H on temperature, despite the large decrease in $[\eta]$ over the range of 25–75 °C. This is a surprising result for which we have no explanation at present.

In summary, it is found that the Flory theory^{11,12} effectively predicts V_2^* for CEHPC from measured values of l' and d . Good agreement is also found for other polymers, with the exception of HPC which shows more complicated behavior. A large negative temperature coefficient is found for CEHPC in agreement with behavior observed for other cellulose derivatives.

Acknowledgment. The author thanks Dr. P. E. Barnum for preparing the CEHPC sample, Dr. N. P. Pyrras for X-ray diffraction measurements, and Dr. B. J. Swetlin for initiating interest in this work. Critical readings of the paper by Dr. J. S. Lindner and Dr. L. J. Fetters are also gratefully acknowledged.

Registry No. CEHPC, 37291-33-1.

References and Notes

- (1) Present address: Department of Chemistry, University of Alabama at Birmingham, Birmingham, AL 35294.
- (2) Werbowyj, R. S.; Gray, D. G. *Mol. Cryst. Liq. Cryst.* **1976**, *34*, 97.
- (3) Werbowyj, R. S.; Gray, D. G. *Macromolecules* **1980**, *13*, 69.
- (4) Bheda, J.; Fellers, J. F.; White, J. L. *Colloid Polym. Sci.* **1980**, *258*, 1335.
- (5) Onogi, Y.; White, J.; Fellers, J. *J. Non-Newtonian Fluid Mech.* **1980**, *7*, 121.
- (6) Chanzy, M.; Peguy, A. *J. Polym. Sci., Polym. Phys. Ed.* **1980**, *18*, 1137.
- (7) Aharoni, S. M. *Mol. Cryst. Liq. Cryst.* **1980**, *56*, 237.
- (8) Hudson, S. M.; Cuculo, J. A. *J. Polym. Sci., Polym. Chem. Ed.* **1980**, *18*, 3469.
- (9) Navard, P.; Haudin, J. M.; Dayan, S.; Sixou, P. *J. Polym. Sci., Polym. Lett. Ed.* **1981**, *19*, 379.
- (10) Patel, D. L.; Gilbert, R. D. *J. Polym. Sci., Polym. Phys. Ed.* **1981**, *19*, 1449.
- (11) Flory, P. J. *Adv. Polym. Sci.* **1984**, *59*, 1.
- (12) Flory, P. J. *Proc. R. Soc. London, A* **1956**, *A234*, 73.
- (13) Kratky, O.; Porod, G. *Recl. Trav. Chim. Pays-Bas* **1949**, *68*, 1106.
- (14) Benoit, H.; Doty, P. *J. Phys. Chem.* **1953**, *57*, 958.
- (15) Peterlin, A. *J. Polym. Sci.* **1950**, *58*, 473.
- (16) Peterlin, A. *J. Chem. Phys.* **1960**, *33*, 1799.
- (17) Eizner, Y. E.; Ptitsyn, O. B. *Vysokomol. Soedin.* **1962**, *4*, 1725.
- (18) Hearst, J. E. *J. Chem. Phys.* **1963**, *38*, 1062; **1965**, *42*, 4149.
- (19) Kurath, S. F.; Schmitt, C. A.; Bachhuber, J. J. *J. Polym. Sci., Part A* **1965**, *3*, 1825.
- (20) Yamakawa, H.; Fujii, J. *Macromolecules* **1974**, *7*, 128.

- (21) Yamakawa, H.; Yoshizaki, T. *Macromolecules* 1980, 13, 633.
- (22) Bohdanecky, M. *Macromolecules* 1983, 16, 1483.
- (23) Reddy, G. V.; Bohdanecky, M. *Macromolecules* 1987, 20, 1393.
- (24) Lemieux, R. U.; Purves, C. B. *Can. J. Res., Sect. B* 1947, 25B, 485.
- (25) Wirick, M. G.; Waldman, M. H. *J. Appl. Polym. Sci.* 1970, 14, 579.
- (26) Ambler, M. R.; McIntyre, D. J. *Polym. Sci., Polym. Lett. Ed.* 1975, 13, 589.
- (27) Ambler, M. R.; Fetters, L. J.; Kesten, Y. *J. Appl. Polym. Sci.* 1977, 21, 2439.
- (28) It is, however, possible to obtain fractions with greater polydispersities than that of the parent material in the absence of "cross-fractionation". See: Koningsveld, R. *Pure Appl. Chem.* 1969, 20, 271.
- (29) Flory, P. J. *Principles of Polymer Chemistry*; Cornell University: Ithaca, NY, 1953; Chapter XIII.
- (30) Kurata, M.; Tsunashima, Y.; Iwama, M.; Kamada, K. In *Polymer Handbook*, 2nd ed.; Brandrup, J., Immergut, E. H., Eds.; Wiley-Interscience: New York, 1975; Section IV.
- (31) Reference 29, pp 311-13.
- (32) Marchessault, R. R.; Sarko, A. *Adv. Carbohydr. Chem.* 1967, 22, 445.
- (33) Flory, P. J.; Spurr, O. K., Jr.; Carpenter, D. K. *J. Polym. Sci.* 1959, 27, 231.
- (34) Kamide, K.; Miyazaki, Y. *Polym. J.* 1978, 10, 409.
- (35) Kamide, K.; Saito, M. *Polym. J. (Tokyo)* 1986, 18, 569.
- (36) Norisuye, T.; Fujita, H. *Polym. J. (Tokyo)* 1982, 14, 143.
- (37) Also, no exact model for chain packing was assumed since insufficient information was available to allow a reliable choice of models to be made. The d spacing at 15.2 Å was assumed to correspond to a first approximation with the chain diameter.
- (38) Laivins, G. V.; Gray, D. G. *Macromolecules* 1985, 18, 1746.
- (39) Laivins, G. V.; Gray, D. G. *Macromolecules* 1985, 18, 1753.
- (40) Conio, G.; Bianchi, E.; Ciferri, A.; Tealdi, A.; Aden, M. A. *Macromolecules* 1983, 16, 1264.
- (41) Aden, M. A.; Bianchi, E.; Ciferri, A.; Conio, G.; Tealdi, A. *Macromolecules* 1984, 17, 2010.
- (42) Tanner, D. W.; Berry, G. C. *J. Polym. Sci., Polym. Phys. Ed.* 1974, 12, 941.
- (43) Goebel, K. D.; Harvie, C. E.; Brant, D. A. *Appl. Polym. Symp.* 1976, 2, 671.

Fatigue Behavior of Ionomers. 1. Ion Content Effect on Sulfonated Polystyrene Ionomers

Masanori Hara,* Pean-Yue Jar, and J. A. Sauer

Department of Mechanics and Materials Science, Rutgers, The State University of New Jersey, Piscataway, New Jersey 08855-0909. Received December 15, 1987; Revised Manuscript Received April 20, 1988

ABSTRACT: Fatigue properties of sulfonated polystyrene ionomers were studied as a function of ion content. It was found that the fatigue performance of ionomers decreased with ion content up to ca. 5 mol %. This was attributed to the cross-linking effect of small ionic aggregates (multiplets). The fatigue lifetime increases sharply at ca. 5 mol %, which corresponds to the critical ion content of polystyrene-based ionomers. This increase in fatigue performance is related to the dominant role of large ionic aggregates (clusters). Finally, the fatigue performance of the ionomers increased gradually with ion content, a result attributed to the reinforcing filler effect of the clusters. The fatigue fracture surface morphologies observed by scanning electron microscopy are discussed.

Introduction

It is widely recognized that the introduction of ions into organic polymers modifies their properties dramatically. For example, the glass transition temperature of polyphosphate rises from -10 °C for the nonionic polyacid to +520 °C for the calcium polyphosphate.¹ Many examples of large changes in properties are cited in recent books and reviews.¹⁻⁵ Therefore, the introduction of ionic groups into polymer chains has become an interesting and useful approach to modifying the various properties of polymers.

Ionomers are a relatively new class of ion-containing polymers which have ions in concentration up to 10-15 mol %, distributed in nonionic backbone chains. Since the development of ionomers (Surlyn) by DuPont in 1966,⁶ ionomers have caught the attention of people in both industry and academia. This is again based on the fact that the incorporation of ions into solid polymers frequently leads to profound changes in properties, such as glass transition temperature and melt viscosity. Much work has been devoted to elucidating the overall structure-property relationships of ionomers. It has been found that the change in properties of ionomers in the solid state is due to the clustering of ion pairs in the medium of low dielectric constant.¹⁻³ Two types of ionic aggregates are proposed to exist according to ion content:¹ (1) below a certain ion content, multiplets consisting of a small number of ion pairs, which work as physical cross-links, dominate;

(2) above that critical ion content, larger aggregates (clusters) consisting not only of ion pairs but also of portions of hydrocarbon chains, which bear many of the characteristics of microphase separation, dominate.

Although much work has been done to elucidate the structure-property relationship of ionomers, most of the properties so far discussed relate to the regions above the glass transition. Such properties as the glass transition temperature, the high-temperature modulus, and the melt viscosity have been determined.¹⁻³ Little work has been reported in the literature about the glassy state properties, such as yield behavior, impact strength, fatigue behavior, etc., although real use of ionomers as engineering plastics is indeed in the glassy state.

Over recent years there has been a significant increase in interest in the deformation and fracture behavior of glassy polymers.^{8,9} One of the reasons is the increasing use of plastics in structural engineering applications. We need to understand the way polymers respond to mechanical deformation, especially, their ultimate properties, to use them for load bearing application. Another reason is that it has become possible recently to achieve some understanding of the deformation/fracture behavior from the microstructure viewpoint.¹⁰

In this paper, we report the fatigue properties of ionomers. In recent years, considerable attention has been given to the performance of polymers under cyclic loading